OPEN

PRS GLOBAL OPEN

ORIGINAL ARTICLE
Reconstructive

Noncontrast Magnetic Resonance Imaging of Perforators for Preoperative Evaluation of Anterolateral Thigh Flaps

Frank R. Chen, BS*
Jona Kerluku, BS†
Douglas Mintz, MD†
Alissa J. Burge, MD†
Aaron Z. Chen, BA*
Aoife MacMahon, BA*
Daniel A. Osei, MD, MSc‡
Duretti T. Fufa, MD‡

Background: The anterolateral thigh (ALT) flap is a commonly utilized perforator-based flap in reconstructive surgery. Although previous studies have used various angiographic techniques to preoperatively image ALT perforators, none have investigated the efficacy of noncontrast magnetic resonance imaging (MRI). Our study investigates the efficacy of our institutional fat suppression noncontrast MRI sequence to characterize the number, location, and course of dominant skin perforators in the ALT for preoperative planning.

Methods: We queried our institutional database for 100 noncontrast thigh MRIs from July 2013 to July 2018 that included an axial fat suppression sequence with visualization from the lesser trochanter to the distal musculotendinous junction of the rectus femoris. Perforator course, size, and location relative to bony landmarks were determined.

Results: Of the 100 examinations, 70 included bilateral thighs for a total of 170 thighs for perforator analysis. An estimated 277 perforators were identified, of which 101 were septocutaneous (36.5%) and 176 were musculocutaneous (63.5%). An average of 1.63 perforators were visualized in each thigh (min, 1; max, 4). The average perforator diameter at exit from the anterior thigh compartment fascia was 2.5 mm (SD, 0.5). Perforator exit location along the anterior superior iliac spine- or lesser trochanter-patella line could be determined for n = 57 perforators and mapped into 3 predictable clusters.

Conclusions: At least 1 perforator was found in each of 170 thighs imaged. Perforator course, size, and location measured with noncontrast MRI are consistent with prior literature. Noncontrast MRI is a low-morbidity imaging modality that may serve as an effective tool in preoperative planning of the ALT flap.
(Plast Reconstr Surg Glob Open 2020;8:e3174; doi: 10.1097/GOX.0000000000003174; Published online 22 October 2020.)

INTRODUCTION

Perforator-based fasciocutaneous flaps such as the anterolateral thigh (ALT) flap are versatile and are increasingly utilized in reconstructive surgery. Since it was first described by Song et al in 1984, the ALT flap has emerged as a workhorse flap for soft tissue reconstruction of the head and neck, extremities, and groin because it has minimal donor site morbidity, a long and sizeable pedicle, and provides desirable skin and fascia for coverage.[1–6] The ALT Flap is harvested in the region between the anterior superior iliac spine (ASIS) and the superolateral patella. An incision is made along the rectus femoris and the surrounding tissue is dissected until the perforating vessels supplying the ALT flap can be exposed. The perforating vessels are then dissected to their proximal origins in the lateral circumflex femoral (LCFA) system, resulting in a mean pedicle length of 12 cm, although the size may vary according to the flap design.[7,8]

The perforating vasculature supplying the cutaneous territory of the ALT is highly variable and perforators must be carefully dissected using a meticulous technique to avoid damage. Familiarity with the variable anatomy

*From the *Weill Cornell Medical College, New York, N.Y.; †The Hospital for Special Surgery Department of Radiology, The Hospital for Special Surgery, New York, N.Y; and ‡The Hospital for Special Surgery Department of Hand and Reconstructive Surgery, The Hospital for Special Surgery, New York, N.Y.*

Received for publication May 12, 2020; accepted August 14, 2020.

Presented at International Federation of Societies for Surgery of the Hand 2019, Berlin, Germany.

DOI: 10.1097/GOX.0000000000003174

Disclosure: *The authors have no financial interests to declare in relation to the content of this article.*

and with surgical techniques of intramuscular perforator dissection is critical for flap survival. In a majority of cases, the perforator supply to the ALT originates from the descending branch of the LCFA but, in some cases, perforators originate from the oblique, transverse, or ascending branches of the LCFA.[9] Perforators to the ALT are also variable in course and can travel through muscle (musculocutaneous) or through the intermuscular septum (septocutaneous) before exiting the fascia.[10] Septocutaneous perforators can be more easily exposed between the rectus femoris and vastus lateralis, while musculocutaneous perforators are more technically demanding and time-consuming to dissect safely. In some cases, it has been reported that no perforating vessels from the descending branch could be identified during flap harvest, requiring abandonment of the ALT for an alternative flap donor.[11]

Identification of suitable perforators and determination of perforator characteristics facilitates preoperative planning. Various techniques are used in preoperative evaluation of the ALT to determine perforator location, course, and branching pattern. Two commonly employed, nonimaging techniques used to localize perforators include handheld pencil Doppler ultrasound (commonly referred to as Doppler) and the ABC system described by Yu and Youssef, in which the letters A, B, and C describe the three different positions of perforator exit.[12] Color Doppler ultrasound is another informative type of imaging in which colors are superimposed on moving blood and can indicate the direction and speed in which blood is flowing. This can reliably identify areas of high blood flow and can help identify perforators. Doppler and the ABC system can localize perforators but do not provide information about perforator course, size, or branching pattern. Scanning with Doppler starts halfway along the line between the ASIS and patella (A-P line), and perforators are marked along the A-P line. Although Doppler is sensitive and accurate in thin patients, it is less reliable in obese patients.[12,13] Yu and Youssef's ABC system does not require imaging or Doppler to determine perforator location.[12] Based on a study of 100 free ALT flaps over a 2-year period, Yu and Youssef[12] found that 3 perforators (A, B, and C) can be routinely identified using mini-Doppler. They found that the B midpoint perforator is 1.5 cm lateral to the midpoint of the A-P line and that A and C perforators are 5 cm proximal and distal to the B perforator.[12] Although these are excellent techniques used to facilitate localization of perforators, they do not provide information about perforator size, course, or branching pattern.

Compared with using the Doppler or the ABC system, preoperative imaging of the ALT may be more useful because it provides this additional information beyond perforator number and location, including branching pattern (originating from the transverse, oblique, or descending branches), course (septocutaneous versus musculocutaneous), and size. Imaging techniques that allow for visualization of perforating vessels in the ALT include digital subtraction angiography, computed tomography angiography (CTA), and magnetic resonance angiography (MRA).[14,15] All of these techniques require contrast injection, which poses the risks of vascular damage, renal damage, and allergic reactions.[16,17] Contrast medium may also has a vasoconstricting effect, decreasing the accuracy of vascular diameter and small-caliber vessel course assessment.[17] Additional disadvantages of digital subtraction angiography include its radiation exposure and inability to visualize muscles, nerves, and fat.[16,18] Radiation exposure is also a limitation of CTA, which has been used to visualize the ALT in other studies.[10]

Noncontrast magnetic resonance imaging (MRI) circumvents the risks of radiation and contrast injection and has previously been used to visualize vasculature in abdominal perforator flaps for breast reconstruction.[19] For ALT visualization, previous studies have supported CTA with contrast as the preferred imaging modality because it can show origin vessels, length, and perforator type the most clearly.[2] However, no prior studies have investigated the efficacy of using noncontrast MRI in assessing perforators of the ALT. The primary aim of this study was to investigate the efficacy of our institutional fat-suppression noncontrast MRI sequence to characterize the number, location, and course of skin perforators to the ALT flap.

METHODS

Our institutional database was queried from July 2013 to July 2018 for 100 consecutive noncontrast thigh MRI examinations (70 bilateral) that included an axial fat suppression sequence, with visualization of the region from the lesser trochanter (LT) to the distal musculotendinous junction of the rectus femoris. All patients underwent MRI on a 1.5 or 3.0 T clinical scanner (GE Healthcare, Waukesha, Wis.) utilizing a body or cardiac coil, with the patient scanned in the supine position. These scans were ordered for a variety of indications, but all protocols consisted of coronal and axial fat-suppressed fluid sensitive images (inversion recovery), iterative decomposition of water and fat with echo asymmetry and least-squares estimation, or T2 fat saturation (T2FS) plus axial, sagittal, and coronal proton density weighted fast spin echo images. For dedicated perforator scans, high-resolution unilateral T2FS images were performed for the extremity of interest. Owing to the variable scan indications, parameters were also variable. Predominant slice thickness ranged from 4 to 8 mm with no gap, and the field of view ranged from 14 to 40 cm. Scans of axial inversion recovery consisted of a lower resolution 256 × 192 matrix, while higher resolutions for unilateral T2FS axials were achieved at a 512 × 320 matrix. We excluded thigh MRIs with contrast as well as those that did not capture the region from the lesser trochanter to the distal musculotendinous junction of the rectus femoris, as these landmarks were necessary references for determining perforator exit points. In addition, studies with excessive edema, fatty infiltration, scarring, or artifact that precluded reliable visualization of perforators were also excluded.

Patient demographics were recorded, including age, sex, and indication for thigh MRI (Tables 1, 2). All noncontrast MRIs were downloaded from our institutional picture and archiving communication system and analyzed with OsiriX (Pixmeo SARL, Geneva). Images were converted to 3-dimensional multiplanar reconstructions to visualize the axial and coronal planes of perforators exiting the fascia.

Table 1. Patient Demographics

	Female (n = 58)	Male (n = 42)	Overall (n = 100)
Age, y			
Mean	46	44	45
SD	20	21	21
BMI			
Mean	25.12	26.01	25.49
SD	6.91	4.27	5.95

Table 3. Perforator Characteristics

Total No. patients	100
Total No. thighs	170
Total No. perforators	277 (100%)
Septocutaneous perforators	101 (36.46%)
Musculocutaneous perforators	176 (63.54%)
Average No. perforators per leg	1.63 (range, 1–4)
Diameter of perforator exit from fascia, mm	2.53 (SD, 0.50)
Median site of perforator exit relative to ASIS-patella distance (n = 22 perforators)	0.5

Perforator characteristics were identified on the axial sequence. Attention was focused on the subcutaneous fat layer where visible perforators were traced retrograde to the fascia back to their source vessel. Perforator location, size at the fascia, and course were recorded (Table 3).

Averages and SDs were measured for patient demographics and perforator characteristics. Perforator course, size, and location relative to the ASIS, LT, and patella were determined. Perforators that coursed entirely through the intermuscular septum between the rectus femoris and vastus lateralis were classified as septocutaneous. Perforators that coursed either entirely through muscle or through both the intermuscular septum and muscle before exiting the fascia were classified as musculocutaneous.[10] The site of perforator exit through anterior thigh fascia relative to the LT was measured for all perforators. For those patients who had the ASIS, LT, and patella included on a single examination in X-ray imaging, the ASIS-patella distance was measured from the ASIS to the superior pole of the patella. For these patients, the site of perforator exit through fascia relative to the ASIS-patella distance was calculated based on the ASIS-LT and LT-patella distances. A k-means clustering analysis using R package ggplot2 was performed on identified perforators along the LT-patella line, with sites of perforator exit partitioned into 3 clusters based on the ABC system.[20–23] Descriptive statistics were also utilized to characterize the number, size, course, and location of perforators. A 2-sample Student's *t* test was run to determine differences between perforators in each leg of patients with bilateral thighs on imaging (Table 4). These data were analyzed with a significance threshold of $P = 0.05$.

RESULTS

The study period included examinations performed between July 2013 and July 2018. A total of 100 patient studies were included, with 70 bilateral thigh studies for a total of 170 thighs analyzed. Noncontrast fat-suppressed MRIs for 100 patients (58 women and 42 men) met our inclusion and exclusion criteria and were analyzed. The average patient age in the cohort was 45 (range, 5–81), with 58% women and 42% men; the average BMI was 25.49 (range, 15.1–48.6). Patient demographics are presented in Table 1. Sample noncontrast MRI algorithms based on scan indication are presented in Table 2.

An average of 1.63 perforators were identified per thigh (range, 1–4). An estimated 277 perforators in 170 thighs were identified and classified as either septocutaneous or musculocutaneous. In total, 101 of 277 total perforators were identified as taking a septocutaneous course to the skin (36.5%), while musculocutaneous perforators were identified in 176 of 277 total perforators (63.5%). All included perforators were able to be traced back to their origin from the descending branch of the LFCA. All perforators could be traced back through the fascia and into the muscle or septum. A septocutaneous perforator is shown in Figure 1 and a musculocutaneous perforator is shown in Figure 2.

The average perforator diameter at exit through the anterior thigh fascia was 2.5 mm (SD, 0.5). The A-P distance was found in 9 patients, 14 thighs with n = 22 perforators who had coronal XRs, which included the ASIS and patella. The LT-patella distance was found in 12 additional patients with a combined n = 59 perforators. All measured perforators along the LT-patella line (n = 35) were analyzed through a k-means cluster algorithm. This analysis revealed 3 clusters with an average silhouette of 0.55. The cluster closest to the LT consisted of 16 perforators, cluster closest to the patella consisted of 8 perforators, and 11 perforators grouped in between (Fig. 3).

There were 70 studies in which bilateral thigh examinations were obtained, and of these studies, 113 perforators were identified in the right leg, and 112 perforators were identified in the left leg. There were no statistically significant differences in the number, course, size, and location of perforators between legs (Table 4). The number of perforators was the same on the 2 sides in 53% (37/70) of patients, with an average of 1.61 (SD, 0.64) and 1.60 (SD, 0.67) perforators in the right and left legs, respectively ($P = 0.928$). Of the 37 patients in which the number of perforators were the same in each leg, the course of all perforators (septocutaneous/musculocutaneous) was identical on both sides in 59% (22/37) of patients. Perforator size was within 1 mm

Table 2. Patient MRI Algorithms

Indication	Coverage	Fat-suppressed Fluid Sensitive		Morphologic	
Hamstring injury	Bilateral thighs, lower pelvis	Coronal and axial IR or IDEAL	Axial PD	Coronal PD	
Myositis	Bilateral thighs, lower pelvis	Coronal and axial IR or IDEAL	Axial PD	Coronal PD	Coronal T1
Dedicated ALT	Unilateral thigh	Axial T2FS	Axial PD		

IDEAL, iterative decomposition of water and fat with echo asymmetry and least-squares estimation; IR, inversion recovery; PD, proton density; T2FS, T2 fat saturation.

Table 4. Similarities in Perforators Found in Studies with Both Left and Right Thighs (n = 70 Patients)

Perforator Characteristic	Right Thigh	Left Thigh	*P*
Average No. perforators per thigh	1.61 (SD, 0.64)	1.60 (SD, 0.67)	0.928
Average No. septocutaneous perforators	0.60 (SD, 0.62)	0.57 (SD, 0.62)	0.775
Average No. musculocutaneous perforators	1.01 (SD, 0.77)	1.02 (SD, 0.87)	0.943
Size, mm	2.65 (SD, 0.39)	2.65 (SD, 0.39)	0.976
Location of perforator exit between ASIS-patella (5 studies)	0.50 (SD, 0.07)	0.51 (SD, 0.09)	0.837

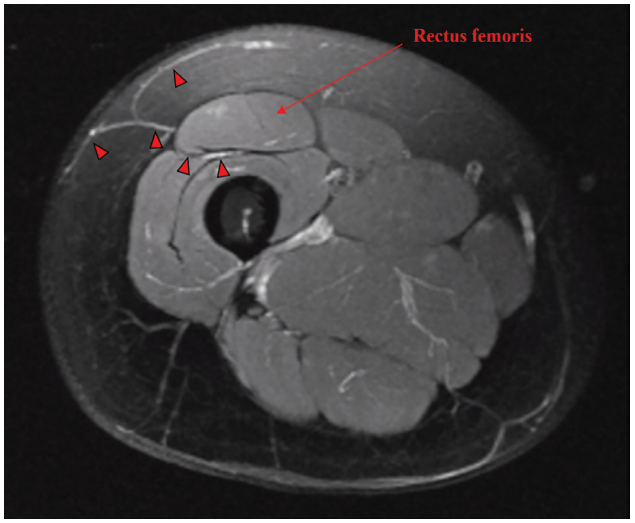

Fig. 1. Noncontrast axial T2 fat-suppressed slabbed maximum intensity projection image of the right thigh in a 21-year-old woman for evaluation of anterolateral thigh perforator anatomy before surgery, demonstrating the course of a prominent septocutaneous perforator (red arrowheads) arising from the descending branch of the lateral circumflex femoral artery.

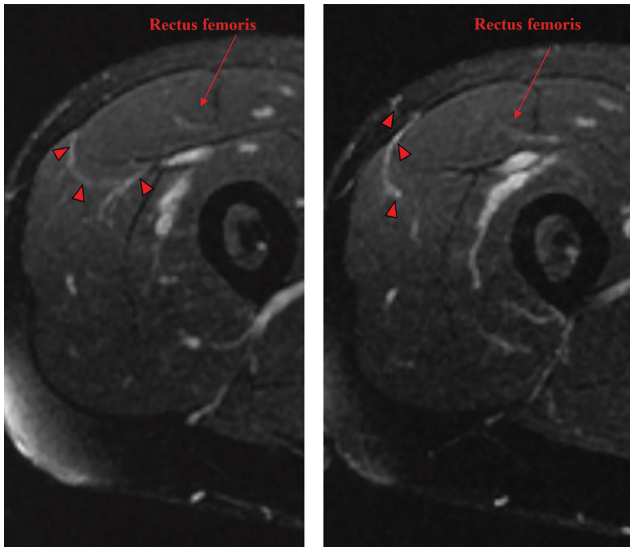

Fig. 2. Noncontrast MRI axial T2 fat-suppressed slabbed maximum intensity projection images of the thigh in a 43-year-old man for evaluation of anterolateral thigh perforator anatomy before surgery, demonstrating the course of a prominent musculocutaneous perforator (red arrowheads) arising from the descending branch of the lateral circumflex femoral artery.

bilaterally in 100% (37/37) of the cases in which the number of perforators was the same in each leg. In the subset of patients with bilateral thighs and measurable A-P distances (5 cases), the relative locations of perforator exit along the ASIS-patella line in the right and left leg were 0.50 (SD, 0.07) and 0.51 (SD, 0.09), respectively ($P = 0.837$).

Case Example

We describe a case in which perforator locations determined by preoperative noncontrast MRI correlated well with Doppler and intraoperative findings. In addition, noncontrast MRI detected excessive edema in

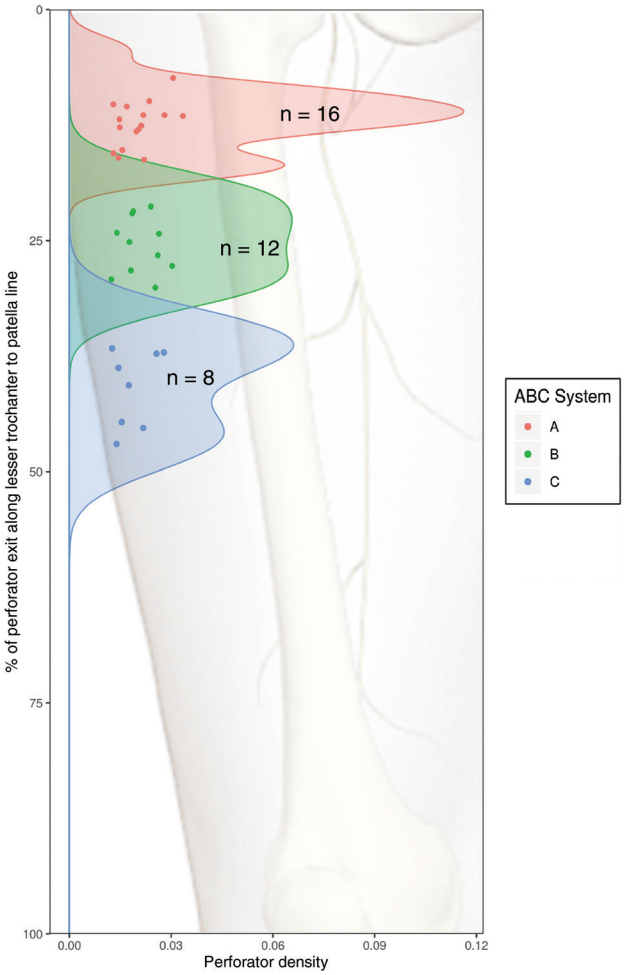

Fig. 3. K-means cluster analysis showing sites' density of perforator exit between the LT and patella determined by a noncontrast MRI for n = 35 perforators. Skeleton adapted from Primal Pictures Anatomy.tv.

the intended limb for ALT transfer that was not appreciable on physical examination and was not detected by Doppler or the ABC system. Because of this, we preoperatively decided to harvest from the contralateral limb. In this case, preoperative imaging potentially spared a challenging or impossible attempted harvest from the original limb that would not otherwise have been detected until intraoperatively.

Clinical History

We now describe the case of a 65-year-old man with a history of a left total knee replacement and revision, prosthetic joint infection treated with incision and drainage and a gastrocnemius rotational flap, who recently underwent explantation and reimplantation of the chronically infected left knee arthroplasty. The patient was then presented to the hospital with a draining wound. A physical examination of the patient revealed active drainage through a knee wound. Wound drainage was initially treated by the primary team with irrigation and debridement, with the inability to primarily close the wound.

Indications for ALT Flap

The patient was then indicated for free ALT flap grafting to the lower leg for resurfacing as part of an attempt to salvage the knee implant. This decision for more aggressive treatment was made due to the presence of a chronic, open lateral wound and the failure of a local rotational flap to manage his skin condition.

Imaging

Bilateral noncontrast thigh MRI was obtained preoperatively to evaluate the suitability of perforators for transfer. Ipsilateral (left) imaging demonstrated a substantial edema in both the thigh musculature and subcutaneous fat that was not appreciated on the physical examination (Fig. 4A). As a result, the decision was made to harvest from the contralateral (right) ALT. Noncontrast MRI of the contralateral ALT revealed 3 perforators. One musculocutaneous perforator is shown in Figure 4B. The relationship between the corresponding predicted MR and surface Doppler perforators are shown further in Figures 5 and 6.

Surgical Course

Preoperative left lower extremity wound drainage and eventual dissection are shown in Figure 5A. The expected perforator location along the ALT thigh, as determined by MRI, Doppler, and the ABC system, is shown in Figure 5B. Intraoperatively, 2 perforators were initially identified as proximal musculocutaneous and distal septocutaneous. During further development of the $12 \times 24\,cm^2$ flap, an additional septocutaneous perforator was identified, confirming the number of perforators seen on preoperative imaging. In all, we found that there was a good correlation between the perforator location as determined by a handheld Doppler versus the perforator location as determined by an MRI (Fig. 6A).

Postoperative Course and Conclusions

His further postoperative course remained uneventful without any flap complication (Fig. 6B). This case illustrates that (1) a preoperative MRI provided information about excessive soft tissue trauma not appreciable by physical examination, leading to decision to harvest from the contralateral limb, (2) perforators discovered on MRI can be reliably identified during surgery, and (3) perforator

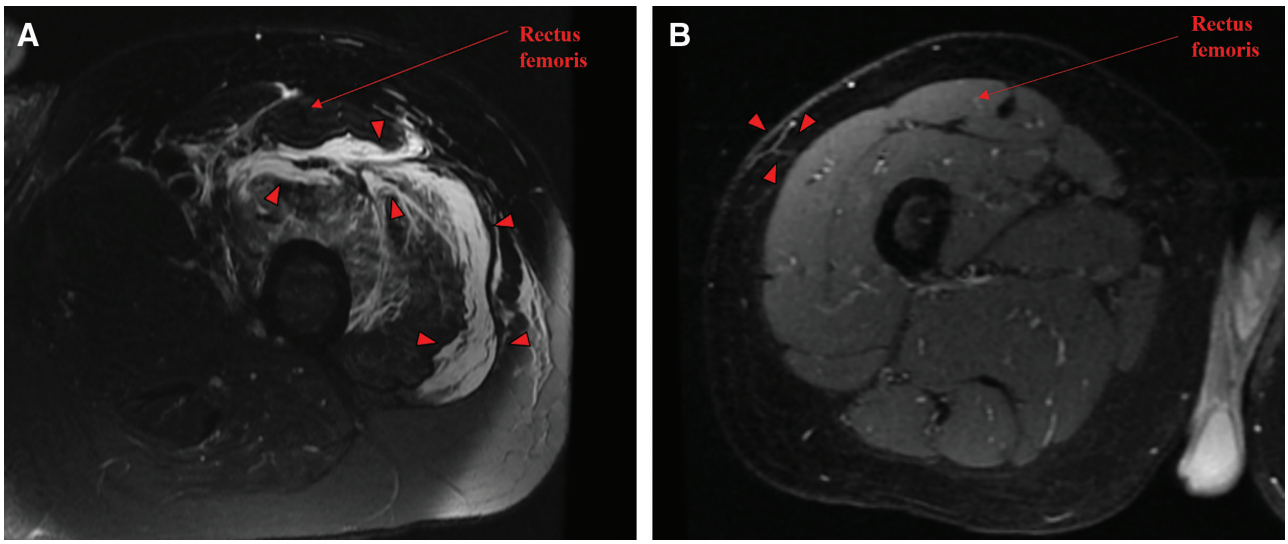

Fig. 4. Non-contrast MRI images of the anterolateral thigh. A, Noncontrast MRI axial T2 fat-suppressed slabbed maximum intensity projection images of the left thigh in a 65-year-old man for evaluation of anterolateral thigh perforator anatomy before surgery, demonstrating a substantial edema in both the thigh musculature and subcutaneous fat (red arrowheads) that was not appreciated on the physical examination. B, Noncontrast MRI axial T2 fat-suppressed slabbed maximum intensity projection images of the contralateral (right) thigh in a 65-year-old man for evaluation of anterolateral thigh perforator anatomy before surgery, demonstrating a musculocutaneous perforator (red arrowheads) that has exited the fascia.

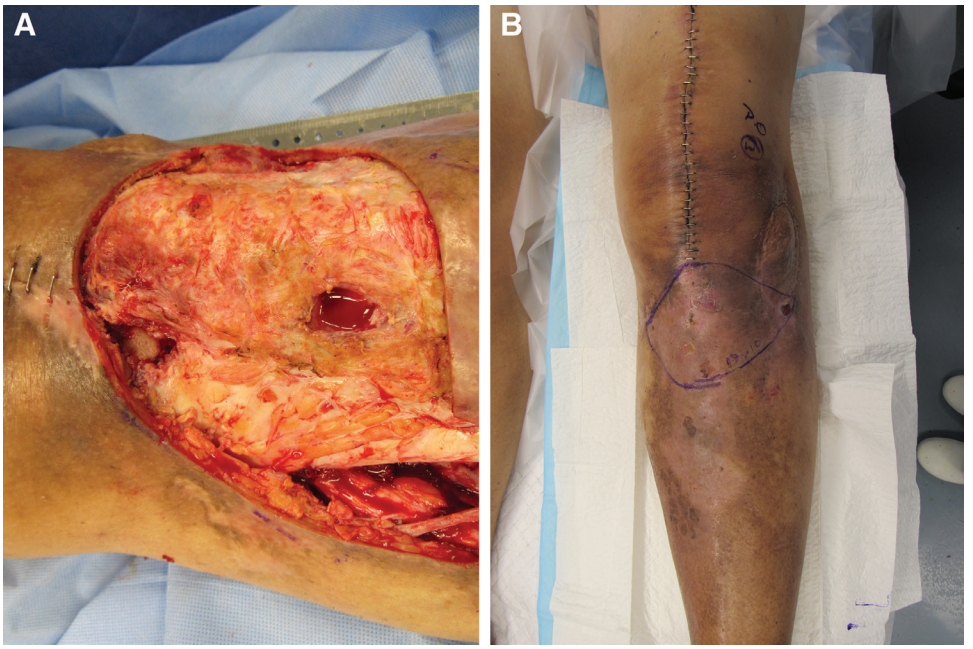

Fig. 5. Preoperative, intraoperative, and postoperative images of the anterolateral thigh. A, Intraoperative picture of the perforator that was harvested. B, Picture of the left lower extremity at follow-up after the surgery.

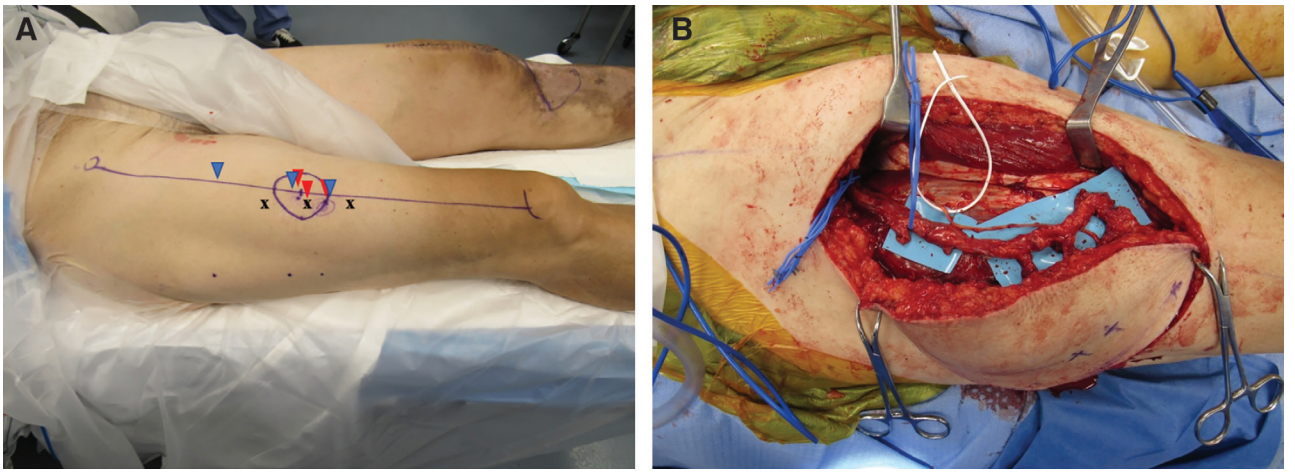

Fig. 6. Photographs and the perforators harvested from the anterolateral thigh region. A, Photograph of the preoperative skin deficiency. Blue triangles indicate the perforator location on the A P line by MRI. Red arrowheads show the perforator location, as determined by the handheld Doppler. X shows the expected location of perforators based on the ABC method. B, Intraoperative photograph of the perforator that was harvested.

location and course determined by MRI correlates well with Doppler and operative findings.

DISCUSSION

In this study, we report the efficacy of using our institutional noncontrast MRI technique to image the perforators supplying the ALT flap. A prior investigation using a noncontrast MRI to image the ALT is limited. In this study, we found at least 1 ALT perforator present in each of the 170 thighs imaged using noncontrast MRI. Perforator size and distribution were consistent with prior literature. We found that the majority of perforators took an intramuscular course (63.5%). Because ALT perforators are variable in their location, course, and branching pattern, evaluation of perforators preoperatively may facilitate flap selection, design, and harvest. Although handheld pencil Dopplers and the ABC system can also identify perforator location, they do not provide information about perforator course, size, or branching pattern. While MRA and CTA do provide this information, they introduce contrast or radiation. We have found that our institutional fat-suppression noncontrast MRI technique is a lower-risk

imaging modality compared with CTA or MRA and also provides clinically relevant information that can guide clinical decision-making.

Our perforator measurements closely match those found in other studies. In their systematic review of clinical cases, Lakhiani et al[9] found that septocutaneous perforators were found in 19.8% of total cases. Seth et al[10] found that of their 174 perforators, 33.9% were septocutaneous and 66.1% were musculocutaneous (52.3% musculoseptocutaneous, 13.8% musculocutaneous). In our study, of our 277 perforators, 36.5% were septocutaneous and 63.5% were musculocutaneous. Seth et al,[10] Lakhiani et al,[9] and Kimata et al[24] found that most perforators exited the fascia at the midpoint between the ASIS and the patella. We also found that most perforators exited the fascia halfway between the ASIS and the patella. In addition, perforator size can be measured and perforator course can be classified, providing clinically useful information for the surgeon before and during flap harvest. While higher BMI can lead to increased ALT flap thickness and could potentially preclude reliable clinical evaluation, we were able to consistently identify perforators and perforator characteristics using this noncontrast MRI technique.

Our study has several limitations. As it was purely an imaging-based study, we did not correlate MR perforator characteristics with in vivo findings, as the majority of the MR studies were not obtained as a part of preoperative evaluation for free flap harvest but rather for other indications. As such we cannot report on the accuracy with which these MR characteristics parallel intraoperative findings. Furthermore, we do not present data demonstrating that preoperative imaging has a clinically relevant impact on surgical course or outcome. MRI, as opposed to the handheld Doppler or the use of surface landmarks, carries an increased cost. However, prior literature evaluating preoperative CTA in flaps for breast reconstruction has demonstrated decreased operative times, physician stress, and lower conversion from the perforator to the muscle flap.[25,26] Finally, cost of MRI, technique, and protocol dependence for interpretation are limitations to this modality compared with more traditional preoperative assessment strategies. Depending on the facility, machine, and other factors, this specific noncontrast MRI focusing on the ALT flap can cost several thousands of dollars in the United States. We acknowledge that the high cost of MRI can be a potential guiding factor in choosing a less-expensive option over MRI for preoperative imaging. This could be a potentially important consideration depending on the clinical context. The purpose of this report was not to advocate the use of MRI preoperatively in all cases, but rather to demonstrate its potential use and advantages, specifically, to demonstrate perforator course (intramuscular versus septocutaneous), which may aid in perforator selection for more complex cases.

It has become our institutional protocol to perform preoperative noncontrast MRI for all perforator flaps to aid in surgical planning. We find that noncontrast MRI of the ALT employs high-resolution unilateral images of the extremity of interest. These images should also include the ASIS or patella to localize ALT perforators along the A-P line before dissection. As suggested by the case example, non-contrast MRI imaging helped identify subcutaneous and muscular edema that was not detected with other methods. The additional benefit of not introducing contrast with its vasoconstrictive and nephrotoxic characteristics and eliminating the challenges of timing scans with the contrast reaching the microvasculature are advantages of noncontrast imaging. This modality can be safely and effectively used in patients with renal failure, allergies, or other contraindications for radiation and contrast.

In summary, we found that noncontrast MRI can effectively image perforators and can provide additional information compared to doppler and the ABC system in identifying perforator characteristics. Future studies may compare noncontrast MRI with other techniques, including a more rigorous surgical correlation in terms of accuracy. Given that the percentage of septocutaneous perforators in the ALT flap has previously been reported between 15% and 30%, this result, in particular, should be confirmed with future studies. Future studies may also investigate the concordance of MRI perforator characteristics with intraoperative findings and determine the impact of imaging on clinical outcomes, including surgical time and flap success. Additional algorithms may also be created that can determine the length and tortuosity of intramuscular course such that when more than one perforator can be identified, those with a more direct course can be selected to facilitate flap harvest and minimize the risk of iatrogenic perforator injury.

Duretti T. Fufa, MD
Hospital for Special Surgery
Hand and Reconstructive Surgery
525 East 71st Street, 2nd Floor
New York, NY 10021
E-mail: fufad@hss.edu

REFERENCES

1. Song YG, Chen GZ, Song YL. The free thigh flap: a new free flap concept based on the septocutaneous artery. *Br J Plast Surg*. 1984;37:149–159.
2. Zhang Y, Pan X, Yang H, et al. Computed tomography angiography for the chimeric anterolateral thigh flap in the reconstruction of the upper extremity. *J Reconstr Microsurg*. 2017;33:211–217.
3. Friji MT, Suri MP, Shankhdhar VK, et al. Pedicled anterolateral thigh flap: a versatile flap for difficult regional soft tissue reconstruction. *Ann Plast Surg*. 2010;64:458–461.
4. Yu P. Reinnervated anterolateral thigh flap for tongue reconstruction. *Head Neck*. 2004;26:1038–1044.
5. Yu P, Robb GL. Pharyngoesophageal reconstruction with the anterolateral thigh flap: a clinical and functional outcomes study. *Plast Reconstr Surg*. 2005;116:1845–1855.
6. Yu P, Sanger JR, Matloub HS, et al. Anterolateral thigh fasciocutaneous island flaps in perineoscrotal reconstruction. *Plast Reconstr Surg*. 2002;109:610–616; discussion 617.
7. LoGiudice JA, Haberman K, Sanger JR. The anterolateral thigh flap for groin and lower abdominal defects: a better alternative to the rectus abdominis flap. *Plast Reconstr Surg*. 2014;133:162–168.
8. Shridharani SM, Wang HD, Sacks JM. Pedicled anterolateral thigh flap for vaginal and perineal reconstruction. *Eplasty*. 2013;13:ic14.
9. Lakhiani C, Lee MR, Saint-Cyr M. Vascular anatomy of the anterolateral thigh flap: a systematic review. *Plast Reconstr Surg*. 2012;130:1254–1268.

10. Seth R, Manz RM, Dahan IJ, et al. Comprehensive analysis of the anterolateral thigh flap vascular anatomy. *Arch Facial Plast Surg*. 2011;13:347–354.
11. Kim JW, Kim DY, Ahn KM, et al. Surgical implications of anatomical variation in anterolateral thigh flaps for the reconstruction of oral and maxillofacial soft tissue defects: focus on perforators and pedicles. *J Korean Assoc Oral Maxillofac Surg*. 2016;42:265–270.
12. Yu P, Youssef A. Efficacy of the handheld Doppler in preoperative identification of the cutaneous perforators in the anterolateral thigh flap. *Plast Reconstr Surg*. 2006;118:928–933; discussion 934.
13. Lin SJ, Rabie A, Yu P. Designing the anterolateral thigh flap without preoperative Doppler or imaging. *J Reconstr Microsurg*. 2010;26:67–72.
14. Zhao Z, Yang J, Wang B, et al. [Clinical application of preoperative imaging evaluation in the anterolateral thigh flap transplantation: comparison of computed tomography angiography, digital subtract angiography and magnetic resonance angiography]. *Zhonghua Zheng Xing Wai Ke Za Zhi*. 2015;31:172–175.
15. Smit JM, Klein S, Werker PM. An overview of methods for vascular mapping in the planning of free flaps. *J Plast Reconstr Aesthet Surg*. 2010;63:e674–e682.
16. Singh J, Daftary A. Iodinated contrast media and their adverse reactions. *J Nucl Med Technol*. 2008;36:69–74; quiz 76.
17. Hasebroock KM, Serkova NJ. Toxicity of MRI and CT contrast agents. *Expert Opin Drug Metab Toxicol*. 2009;5:403–416.
18. Jiang C, Lin P, Fu X, et al. Three-dimensional contrast-enhanced magnetic resonance angiography for anterolateral thigh flap outlining: a retrospective case series of 68 patients. *Exp Ther Med*. 2016;12:1067–1074.
19. Masia J, Kosutic D, Cervelli D, et al. In search of the ideal method in perforator mapping: noncontrast magnetic resonance imaging. *J Reconstr Microsurg*. 2010;26:29–35.
20. MacQueen J. Some methods for classification and analysis of multivariate observations. Proceedings of the Fifth Berkeley Symposium on Mathematical Statistics and Probability, Volume 1: Statistics, 281–297; 1967; Berkeley, Calif.: University of California Press. Available at https://projecteuclid.org/euclid.bsmsp/1200512992.
21. R Core Team. *R: A Language and Environment for Statistical Computing*. 2019. Vienna, Austria: R Foundation for Statistical Computing. Available at https://www.R-project.org/.
22. Wickham H. *ggplot2: Elegant Graphics for Data Analysis*. New York, N.Y.: Springer-Verlag; 2016.
23. Maechler M, Rousseeuw P, Struyf A, et al. R Package Cluster: *Cluster Analysis Basics and Extensions. R package version 2.0.8*. 2019.
24. Kimata Y, Uchiyama K, Ebihara S, et al. Anatomic variations and technical problems of the anterolateral thigh flap: a report of 74 cases. *Plast Reconstr Surg*. 1998;102:1517–1523.
25. Rozen WM, Anavekar NS, Ashton MW, et al. Does the preoperative imaging of perforators with CT angiography improve operative outcomes in breast reconstruction? *Microsurgery*. 2008;28:516–523.
26. Fitzgerald O'Connor E, Rozen WM, Chowdhry M, et al. Preoperative computed tomography angiography for planning DIEP flap breast reconstruction reduces operative time and overall complications. *Gland Surg*. 2016;5:93–98.